Chapter 2

ℜeal and Redshift space effects of tangled magnetic fields

---

[1]This chapter is based on the paper: Gopal & Sethi, 2003, J. Ap. & A.,

Summary and the main results of chapter 2

In the post-recombination era, the residual ionization of the matter though small is non-vanishing and hence can support the presence of the magnetic fields. Large-scale magnetic fields if they exist during this era can influence the dynamics of matter by adding the effect of Lorentz force. This can in turn produce observable effects on the matter distribution at the current epoch. We investigated in detail the effects of spatially tangled magnetic fields on the redshift space distribution of matter. In the standard gravitational clustering scenario, the induced peculiar velocities of matter do not have any rotational component i.e they are curl-free vector fields. This directional feature manifests observationally as distortions in the redshift space matter distribution. Tangled magnetic fields of sufficient strength if present will modify the nature of the distortions mainly because they produce curl modes of the velocity field in addition to the compressional modes. The signature of curl modes will not be detectable if they were sourced by early universe magnetic fields since these modes in general decay with time. However for scenarios of low-redshift fields, we find that it might still be possible to detect this signature. We deduced the exact form of the relation between the redshift and real space power spectrum. In addition to the above we also investigated quantitatively the magnetic field induced density power spectrum for two scenarios viz. early universe magnetic fields and low redshift magnetic fields. Assuming a power law distribution for the magnetic field power spectrum as an initial condition, we computed the real space density power spectrum at the current epoch in both the cases and compared it with existing observations.

The main results obtained from this study are:

- ***The presence of magnetic fields increases both the quadrupole as well as the hexadecapole moments of the redshift space power spectrum with the hexadecapole dominating over the quadrupole. This observational feature can be searched for in the existing and upcoming redshift galaxy surveys like 2dF and SDSS which have the potential to probe such features.***

- ***For the scenario in which the magnetic field could have originated at low redshifts, the induced redshift space matter power spectrum has a generic form*** $P(k) \propto k^4$ ***and hence is incompatible with observations.***

2.1 Introduction

Wasserman (1978) pioneered the quantitative study of the effect of large scale magnetic fields on the formation of structures in the universe. They assumed that when the primeval plasma recombines, the Universe is permeated by a stochastic magnetic field that varies on a comoving scale of a galaxy. After recombination, the radiative forces cease to act on matter and the Lorentz force drives compressional and rotational perturbations. They showed that there exists a growing mode in the time evolution of compressional/density perturbations in the linear regime. They estimated that nano-gauss fields could provide initial conditions for density and velocity perturbations which could gravitationally collapse to form galaxies at the present epoch. Wasserman however performed the analysis assuming that the magnetic fields are tangled only on a single length scale or equivalently, the power spectrum of magnetic fields has a delta-function distribution.

A more detailed analysis for the case of a power-law distribution of the magnetic field power spectrum was performed by Kim, Olinto & Rosner (1996). They calculated the density power spectrum in the presence of magnetic fields. In addition to this, they also studied a model incorporating the back-reaction of the fluid to the Lorentz force via the induction equation, which also led them to derive a magnetic Jeans length. Thus according to their analysis, Wassermann's approach is valid for length scales much larger than the magnetic Jeans length and fluid velocities smaller than the Alfven speed.

The statistics of the large-scale distribution of matter is fully characterised by studying the hierarchy of n-point correlation functions. Two-point functions in real and Fourier space remain the most important tools to understand the formation of structures in the universe (see e.g. Peebles 1980). Recently large galaxy surveys like 2dF (Colless et al. 2001) and SDSS (Tegmark et al. 2004) has computed these functions with unprecedented precision. In particular one of the most important results from the 2dF survey is the unambiguous detection of anisotropy in the two-point functions, which is the best statistical evidence of the large scale velocity field (Peacock et al. 2001, Hawkins et al. 2002). The on-going survey Sloan digital sky survey (SDSS) is likely to improve upon this result owing to its larger size (York et al. 2000). The results of 2dF survey show good agreement with the theoretical predictions of variants of CDM models (see e.g. Lahav et al. 2002), in which initial density perturbations are produced at the time of inflation in the very early universe. Larger surveys like the on-going SDSS have the potential to uncover small discrepancy between theory and observations.

In this chapter we study the possibility that initial density and velocity perturbations were caused by tangled magnetic fields. More specifically, we evaluate the density power spectrum in redshift space for two scenarios and compare with present observations. In one

class of models we assume the magnetic fields to have originated in very early universe; we also consider simple models in which the magnetic fields could be of more recent origin and could have originated by astrophysical processes at $z \lesssim 10$. This study could be considered a continuation of early studies of Olinto et al. (1996) who calculated density power spectrum in real space and Sethi (2003) who computed the density two-point correlation function in redshift space.

In the next section we discuss the Magneto-hydrodynamics equations and the evolution of density and velocity fields in the presence of tangled magnetic fields.

In §2.3 we distinguish between real and redshift space quantities and discuss the properties of spatial correlation of the density and velocity fields in both these spaces.

In §2.4 we discuss the properties of the real space power spectrum of the density and velocity fields and compare it with observations.

In §2.5 we summarize our conclusions. For all the calculations described in this chapter, we use the currently-favoured background cosmological model: spatially flat with $\Omega_m = 0.3$ and $\Omega_\Lambda = 0.7$ (Perlmutter et al. 1999, Riess et al. 1998). For numerical work we use $\Omega_b h^2 = 0.02$ (Tytler et al. 2000) and $h = 0.7$ (Freedman et al. 2001).

2.2 Magneto-hydrodynamics Equations

In co-moving coordinates, the equations of magneto-hydrodynamics in the linearized Newtonian theory are (Wasserman 1978):

$$\frac{d(a\mathbf{v}_b)}{dt} = -\nabla\phi + \frac{(\nabla\times\mathbf{B})\times\mathbf{B}}{4\pi\rho_b} \tag{2.1}$$

$$\nabla.\mathbf{v}_b = -a\dot{\delta}_b \tag{2.2}$$

$$\nabla^2\phi = 4\pi G a^2(\rho_{\rm DM}\delta_{\rm DM} + \rho_b\delta_b) \tag{2.3}$$

$$\frac{\partial(a^2\mathbf{B})}{\partial t} = \frac{\nabla\times(\mathbf{v_b}\times a^2\mathbf{B})}{a} \tag{2.4}$$

$$\nabla.\mathbf{B} = 0 \tag{2.5}$$

In Eq. (2.1) the pressure gradient from matter is neglected as it is important at Jeans' length scales ($k \gg 1\,{\rm Mpc}^{-1}$ before re-ionization and $\simeq 1\,{\rm Mpc}^{-1}$ after re-ionization). Our interest here is to study scales at which the perturbations are linear at the present epoch, $\gtrsim 10\,{\rm h}^{-1}$Mpc or $k \lesssim 0.2{\rm hMpc}^{-1}$. Eq. (2.1) and Eq. (2.2) can be combined to give:

$$\frac{\partial^2\delta_b}{\partial t^2} + 2\frac{\dot{a}}{a}\frac{\partial\delta_b}{\partial t} - 4\pi G(\rho_{\rm DM}\delta_{\rm DM} + \rho_b\delta_b) = \frac{\nabla.[(\nabla\times\mathbf{B})\times\mathbf{B}]}{4\pi a^2\rho_b} \tag{2.6}$$

Here the subscript 'b' refers to the baryonic component and the subscript 'DM' refers to the dark matter component. Fluid equations for the evolution of dark matter perturbations can

be obtained from the equations above by dropping the magnetic field terms (Peebles 1980). Wasserman (1978) showed that Eq. (2.6) admits a growing solution, i.e. tangled magnetic fields can provide initial conditions for the growth of density perturbations. These solutions are discussed in the next section. In Eq. (2.4) we have assumed the medium to have infinite conductivity which is valid for the large scales which we consider in the analysis. As a result, we can make a further simplification by neglecting the back-reaction term on the right hand side of the equation as it is of higher order in the perturbed variables,

$$\mathbf{B}(x,t)a^2 = \text{constant}. \tag{2.7}$$

Thus, the magnetic field evolution occurs in a flux-frozen manner without any distortion in the spatial spectrum.

We assume the tangled magnetic field to be a statistically homogeneous and isotropic vector random process. In this case the two-point correlation function of the field in Fourier space can be expressed as (Landau & Lifshitz 1987):

$$\langle B_i(\mathbf{q})B_j^*(\mathbf{k})\rangle = \delta_D^3(\mathbf{q}-\mathbf{k})\left(\delta_{ij} - q_iq_j/q^2\right)B^2(q) \tag{2.8}$$

In addition we assume the tangled magnetic fields to obey Gaussian statistics. This leads to the simplification that all higher even order correlations can be written in terms of the power spectrum.

2.2.1 Time evolution of density and velocity perturbations

The space and time dependence in the solution of Eq. (2.6) can be separated. Eq. (2.6) contains two source terms: dark matter perturbations and tangled magnetic fields. Similar equation for the dark matter perturbations contains baryonic perturbations as the source term.

$$\begin{aligned}
\frac{\partial^2\delta_b}{\partial t^2} &= -2\frac{\dot{a}}{a}\frac{\partial\delta_b}{\partial t} + 4\pi G(\rho_{\rm DM}\delta_{\rm DM} + \rho_b\delta_b) + S(t,x) \\
\frac{\partial^2\delta_{\rm DM}}{\partial t^2} &= -2\frac{\dot{a}}{a}\frac{\partial\delta_{\rm DM}}{\partial t} + 4\pi G(\rho_{\rm DM}\delta_{\rm DM} + \rho_b\delta_b)
\end{aligned} \tag{2.9}$$

Here $S(t,x)$ is the source term from magnetic fields. The dark matter is not directly affected by the magnetic fields. To solve these equations, we define $\delta_{\rm m} = (\rho_{\rm DM}\delta_{\rm DM} + \rho_{\rm b}\delta_{\rm b})/\rho_{\rm m}$ with $\rho_{\rm m} = (\rho_{\rm DM} + \rho_{\rm b})$. This leads to:

$$\begin{aligned}
\frac{\partial^2\delta_b}{\partial t^2} &= -2\frac{\dot{a}}{a}\frac{\partial\delta_b}{\partial t} + 4\pi G\rho_{\rm m}\delta_{\rm m} + S(t,x) \\
\frac{\partial^2\delta_{\rm m}}{\partial t^2} &= -2\frac{\dot{a}}{a}\frac{\partial\delta_{\rm m}}{\partial t} + 4\pi G\rho_{\rm m}\delta_{\rm m} + \frac{\rho_b}{\rho_m}S(t,x)
\end{aligned} \tag{2.10}$$

The second of these equations can be solved by usual Green's function methods. Its solution is:

$$\delta_{\rm m}(x,t) = A(x)D_1(t) + B(x)D_2(t) - D_1(t)\int_{t_i}^{t} dt' \frac{S(t',x)D_2(t')}{W(t')} + D_2(t)\int_{t_i}^{t} dt' \frac{S(t',x)D_1(t')}{W(t')} \tag{2.11}$$

Here $W(t) = D_1(t)\dot{D}_2(t) - D_2(t)\dot{D}_1(t)$ is the Wronskian. $D_1(t)$ and $D_2(t)$ are the solutions of the homogeneous part of the $\delta_{\rm m}$ evolution (Peebles 1980). These terms have the space dependence corresponding to initial, presumably originated during inflation, perturbations. There is no reason to expect that there will be any correlation between these perturbations and the tangled magnetic field-induced perturbations. And therefore in the two-point functions these two contributions will add in quadrature. We only consider magnetic field-induced perturbations for our analysis and drop the first two terms from Eq. (2.11). In Eq. (2.11), t_i corresponds to the epoch of recombination as compressional modes cannot grow before that epoch (see e.g. Subramanian & Barrow 1998). So our initial conditions are: $\delta(t_i) = \dot{\delta}(t_i)$, as is evident from Eq. (2.11). The solution to Eq. (2.11) can be readily calculated analytically for $\Omega_m = 1$ universe (Wasserman 1978). For the currently favoured cosmological model—spatially flat with non-zero cosmological constant—these solutions have to be found numerically. The evolution of $\delta_{\rm b}$ can be solved from:

$$\frac{1}{a^2}\frac{\partial}{\partial t}\left(a^2\frac{\partial \delta_{\rm b}}{\partial t}\right) = \frac{3}{2}H^2\delta_{\rm m} + S(t,x) \tag{2.12}$$

Here we have used: $H^2 = (8\pi G/3)\rho_m$. At high redshifts, solutions to Eq. (2.12) can be found analytically and allow us some insight into the numerical solutions. For $z \gg 1$ the fastest growing solution of Eq. (2.12) is $\propto \Omega_b/\Omega_m^2 t^{2/3}$. It shows that in the presence of the dark matter, perturbations in baryonic matter are suppressed by a factor Ω_b/Ω_m^2.

Tangled magnetic fields give rise to both compressional and curl velocity fields. The time dependence of these two modes is different. The time dependence of the compressional velocity mode v_d can be found from the continuity equation (Eq. (2.2) and Eq. (2.11). For $\Omega_m = 1$ model, the compressional modes grow as $a^{1/2}$. In the presence of dark matter, their growth like the density mode is suppressed by a factor Ω_b/Ω_m^2.

The time evolution of the curl part of the velocity can be found by either taking the curl of Eq. (2.1) or in Fourier space project out the transverse part of the velocity field (see below). The time dependence of the resulting equation is readily solved:

$$\mathbf{v}_c(t) = a(t)^{-1}\int_{t_i}^{t} \frac{dt'}{a^{-3}(t')}\mathbf{S}(t',x) \tag{2.13}$$

$\mathbf{v}_c$ doesn't have any growing mode. In the $\Omega_m = 1$ model $\mathbf{v}_c \propto a^{-1/2}$. Unlike the density and compressional velocity modes it doesn't suffer any suppression in the presence of dark

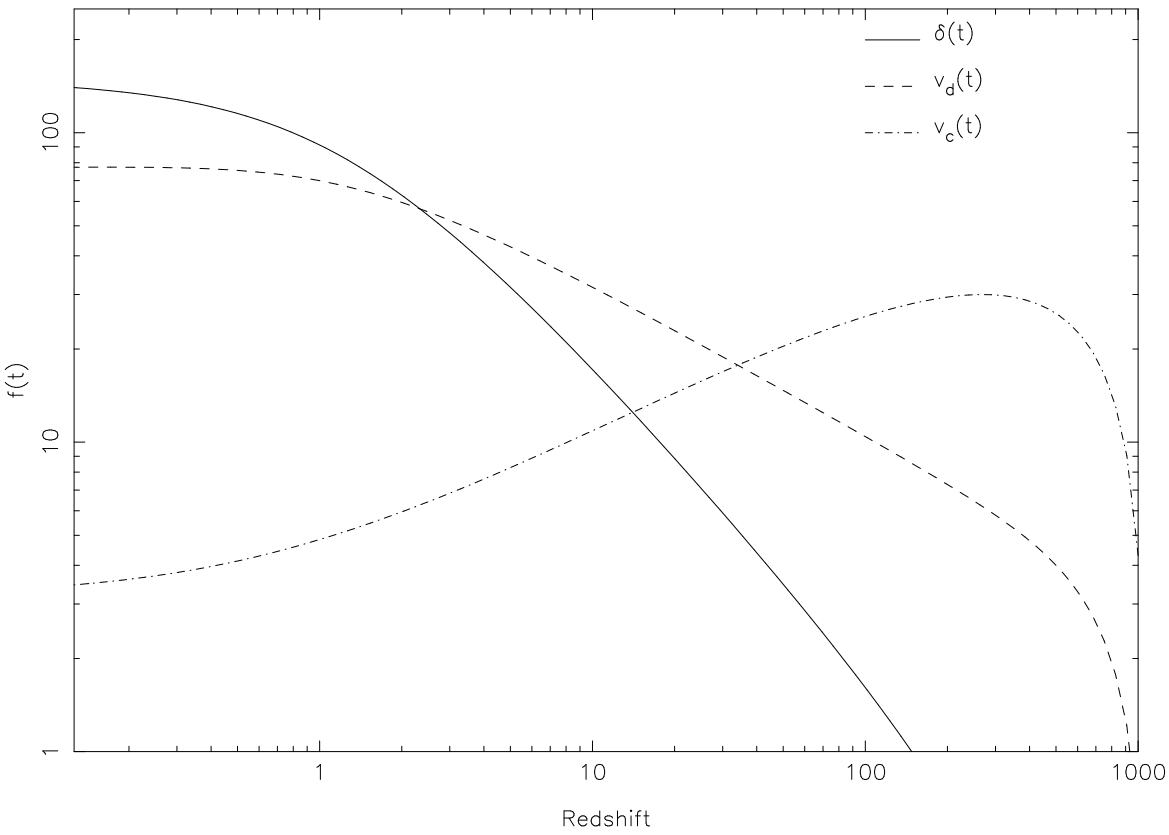

Figure 2.1: Evolution of density and velocity fields is shown if the tangled magnetic fields existed at the last scattering surface.

matter. This is understandable because the only force which couples dark matter and baryons is the gravitational force which is pure gradient and hence does not affect the vortical/curl component of the velocity field.

The time evolution of density and velocity fields is shown in Figure 2.1. In case the tangled magnetic fields originated in the very early universe, the effect of the non-compressional modes generated by the magnetic fields would be negligible on the large scale structure at the present epoch, as these modes would have decayed by the present. Only if the magnetic fields are of more recent origin, these modes could have played an important part in the dynamics of large scale structure.

2.3 Real space and redshift space

The density and velocity fields as described in the previous section are defined as functions of comoving spatial coordinates. Assuming the origin to lie at the observer, we can conveniently fix two of these coordinates as the angular coordinates while the third coordinate is then the radial comoving distance. The angular coordinates of an object can be directly fixed from the observed location in the sky whereas additional information/assumption is required for

determining the third dimension viz. the radial distance. This information exists indirectly in the form of the redshift of the object which is a quantity directly obtained from observations. We can thus distinguish between two spaces viz the real space defined by the comoving coordinates and the redshift space in which the third dimension is the redshift of the object. In a smooth Universe, the real space coordinates and the redshift space coordinates have a one-one mapping such that the redshift z is related to the radial coordinate r by Hubble's law:

$$cz = H_0 r \tag{2.14}$$

The above form of the relation holds for distances less than the size of the horizon at the current epoch. In this case, then, the observed distribution of matter in redshift space directly reproduces the true real space distribution . However, in the presence of density fluctuations, the above mapping gets changed. This is because the density fluctuations induce peculiar velocities, on top of the Hubble flow, resulting in a modified relation:

$$cz = Hr + \mathbf{v}.\hat{\mathbf{r}} \tag{2.15}$$

The velocity field thus contributes an additional redshift through its line-of sight or radial component. In such a case, then, the distribution of matter in redshift space will be related in a non-trivial manner to that in real space. In the next section, we describe the relations between density fields and velocity fields in real and redshift space.

2.3.1 Density and velocity fi elds

The density and velocity fields are statistically homogeneous and isotropic random processes in real space. This allows one to define the power spectrum of the density field, $P(k)$, as (see e.g. Peebles 1980):

$$\langle \delta(\mathbf{k})\delta(\mathbf{k}')\rangle = (2\pi)^3 P(k)\delta_D^3(\mathbf{k}+\mathbf{k}') \tag{2.16}$$

In redshift space both statistical homogeneity and isotropy of the density field break down (see e.g. Hamilton 1998) and in general it is difficult to evaluate the correlations. A simplification can however be made if we treat the lines of sight to two different sources on the sky as parallel which is valid if the sources are far away or the angle between the two lines of sight θ is such that $\theta \ll 1$. This is known as the plane-parallel approximation which was introduced by Kaiser (1987). In the plane parallel approximation , the density field is only statistically anisotropic. This is generally a good assumption in analysing large scale data (Hamilton 1998). We make this assumption in our analysis here. In linear theory and in the plane parallel approximation the observed density field, i.e. the redshift space density field, $\delta^s(\mathbf{r})$ can be written in terms of the real space density and velocity field as:

$$\delta^s(\mathbf{r},t) = \delta(\mathbf{r},t) - \hat{\mathbf{z}}.\nabla\hat{\mathbf{z}}.\mathbf{v}_b(\mathbf{r},t) \tag{2.17}$$

Here $\hat{z}$ is taken to be the common line of sight to all the objects. In Fourier space Eq. (2.17) can be written as:

$$\delta^s(\mathbf{k}, t) = \delta(\mathbf{k}, t) + ik_z v_z(\mathbf{k}, t) \tag{2.18}$$

Here $k_z = \hat{\mathbf{z}}.\mathbf{k}$ and $v_z = \hat{\mathbf{z}}.\mathbf{v_b}$. The velocity field in the case of tangled magnetic fields has both a divergence and a curl component.

$$\mathbf{v_b} = \mathbf{v_d} + \mathbf{v_c} \tag{2.19}$$

Here $\mathbf{v_d}$ and $\mathbf{v_c}$ are the divergence and curl part of the velocity field. Their time evolution is already discussed in the last section. We can rewrite these dependances in the following manner:

$$\delta(\mathbf{r}, t) = f(t)\nabla.[(\nabla \times \mathbf{B}) \times \mathbf{B}] \tag{2.20}$$

$$\mathbf{v_d}(\mathbf{r}, t) = g_1(t)\nabla.[(\nabla \times \mathbf{B}) \times \mathbf{B}] \tag{2.21}$$

$$\mathbf{v_c}(\mathbf{r}, t) = g_2(t)\nabla \times [(\nabla \times \mathbf{B}) \times \mathbf{B}] \tag{2.22}$$

In Fourier space the divergence component points in the direction of the **k** vector, therefore it is convenient to decompose the velocity field parallel and perpendicular to the **k** vector, this gives the velocity field in the Fourier space as:

$$\mathbf{v_d}(\mathbf{k}) = \hat{\mathbf{k}}\hat{\mathbf{k}}.\mathbf{v}(\mathbf{k}) \tag{2.23}$$

$$\mathbf{v_c}(\mathbf{k}) = \mathbf{v}(\mathbf{k}) - \hat{\mathbf{k}}\hat{\mathbf{k}}.\mathbf{v}(\mathbf{k}) \tag{2.24}$$

$\mathbf{v_d}$ can readily be solved in terms of the density field using the continuity equation (Eq. (2.2):

$$\hat{\mathbf{z}}.\mathbf{v}_d(\mathbf{k}) \equiv v_{dz} = -\frac{i\mu}{k}\delta(\mathbf{k})g_1(t) \tag{2.25}$$

Here $\mu = k_z/k$ is the angle between the Fourier mode and the line of sight and $g_1(t)$ is the time dependence of the divergence part of the velocity field; it is shown in Figure 2.1. Note that we use the same symbols for density and velocity fields in both real and Fourier space. The curl part of the velocity field in the Fourier space is projected out by multiplying the Euler equation (Eq. (2.1) by $\delta_{ij} - \hat{k}_i\hat{k}_j$, δ_{ij} being the Kronecker delta function. The time dependence of the curl mode $g_2(t)$ is given in Eq. (2.13) and shown in Figure 2.1.

2.3.2 Redshift space power spectrum

As discussed in the previous section, in redshift space, the density field in general is neither homogenous nor isotropic. However, in the plane-parallel approximation, the density field remains statistically homogenous but anisotropic. The power spectrum in redshift space can then be defined as:

$$\langle \delta^s(\mathbf{k})\delta^s(\mathbf{k}')\rangle = (2\pi)^3 P^s(\mathbf{k})\delta_D^3(\mathbf{k} + \mathbf{k}') \tag{2.26}$$

We thus see that the power spectrum is dependant on the full wave vector as opposed to the dependance only on the magnitude when the condition of isotropy also is satisfied. From Eq. (2.26) and Eq. (1.18) the redshift space power spectrum can be written as:

$$(2\pi)^3 P_s(\mathbf{k},t)\delta_D^3(\mathbf{k}+\mathbf{k}') = \langle(\delta(\mathbf{k},t) + ik_z v_z(\mathbf{k},t))(\delta(\mathbf{k}',t) + ik_z' v_z(\mathbf{k}',t))\rangle \tag{2.27}$$

This can be expanded as:

$$\begin{aligned} P_s(\mathbf{k},t) &= P(k)f^2(t) - g_1(t)k_z^2\langle v_{dz}(\mathbf{k})v_{dz}(-\mathbf{k})\rangle + ig_1(t)f(t)k_z\langle\delta(\mathbf{k})v_{dz}(-\mathbf{k})\rangle \\ &+ ig_1(t)f(t)k_z\langle\delta(-\mathbf{k})v_{dz}(\mathbf{k})\rangle - ig_2(t)f(t)k_z\langle\delta(\mathbf{k})v_{cz}(-\mathbf{k})\rangle \\ &+ ig_2(t)f(t)k_z\langle\delta(-\mathbf{k})v_{cz}(\mathbf{k})\rangle + g_2^2(t)k_z^2\langle v_{cz}(\mathbf{k})v_{cz}(-\mathbf{k})\rangle \\ &+ k_z^2 g_1(t)g_2(t)\langle v_{dz}(\mathbf{k})v_{cz}(-\mathbf{k})\rangle - k_z^2 g_1(t)g_2(t)\langle v_{dz}(-\mathbf{k})v_{cz}(\mathbf{k})\rangle \end{aligned} \tag{2.28}$$

Here $P(k) = \langle\delta(\mathbf{k})\delta(-\mathbf{k})\rangle$ is the real space power spectrum. It is derived in Appendix A. $f(t)$ gives the evolution of density perturbations (Eq. (2.11) and Figure 2.1). The correlations involving the divergence part of the velocity fields can be readily written using the continuity equation (Eq. (2.2):

$$\begin{aligned} \langle\delta(-\mathbf{k})v_{dz}(\mathbf{k})\rangle &= -i\frac{k_z}{k^2}P(k) \\ \langle v_{dz}(\mathbf{k})v_{dz}(-\mathbf{k})\rangle &= -\frac{k_z^2}{k^4}P(k) \end{aligned} \tag{2.29}$$

Eq. (2.29) along with the first four terms of Eq. (2.28) give the usual formula of redshift-distortion first derived by Kaiser (1987): $P_s(\mathbf{k}) = (1+\mu^2\beta)^2 P(k)$, where $\beta = g_1(t_0)/f(t_0) \simeq \Omega_m^{0.6}$ (Lahav et al. 1991). Analysis of 2dF data suggests that $\beta \simeq 0.4$ (Peacock *et al. 2001*). Tangled magnetic fields also generate curl modes, which give rise to additional terms in the power spectrum in redshift space. We show in Appendix A that:

$$\begin{aligned} \langle\delta(-\mathbf{k})v_{cz}(\mathbf{k})\rangle &= 0 \\ \langle v_{dz}(\mathbf{k})v_{cz}(-\mathbf{k})\rangle &= 0 \end{aligned} \tag{2.30}$$

The non-trivial contribution come from the term: $\langle v_{cz}(\mathbf{k})v_{cz}(-\mathbf{k})\rangle$. This can be written as:

$$\langle v_{cz}(\mathbf{k})v_{cz}(-\mathbf{k})\rangle = \langle v_z(-\mathbf{k})v_z(\mathbf{k})\rangle - \frac{k_z^2}{k^4}P(k) + i\frac{k_z}{k^2}\langle v_z(\mathbf{k})\delta(-\mathbf{k})\rangle - i\frac{k_z}{k^2}\langle v_z(-\mathbf{k})\delta(\mathbf{k})\rangle \tag{2.31}$$

In Appendix A we show that, $\langle v_z(\mathbf{k})\delta(-\mathbf{k})\rangle = -ik_z/k^2 P(k)$. This simplifies the equation to:

$$\langle v_{cz}(\mathbf{k})v_{cz}(-\mathbf{k})\rangle = \langle v_z(-\mathbf{k})v_z(\mathbf{k})\rangle + 3\frac{k_z^2}{k^4}P(k) \tag{2.32}$$

The term $\langle v_z(-\mathbf{k})v_z(\mathbf{k})\rangle$ cannot be written in terms of $P(k)$. As shown in Appendix A, it contributes two positive terms proportional to μ^2 (quadrupole) and μ^4 (hexadecapole) with

magnitude comparable to $P(k)$ (Eq. (2.49). This information along with Eq. (2.32) allows us to assess the contribution of the curl component of the velocity field to the redshift space distortion. Its contribution at the present epoch is proportional to $g_2^2(t_0)$. If the magnetic fields originated in the very early universe then the contribution of the curl component of the velocity field is negligible as it doesn't have any growing mode. From Figure 2.1, we can see that $g_2(t_0)/g_1(t_0) \ll 1$. However if the magnetic field have their origin in the recent history of the universe then it is possible to have $g_2(t_0) \simeq g_1(t_0)$. In this case the curl component enhances the contribution in both μ^2 and μ^4 terms. It is interesting to note that unlike the divergence term in which μ^4 term is smaller than the μ^2 term by a factor of $\beta/2$, the curl contribution is dominated by the μ^4 term. In many models we studied it can be nearly 5 times the μ^2 term. The presence of the curl component leads to the intriguing possibility that the observed redshift space distortion is dominated by the curl mode. In that case it is not possible to infer the value of β from this observation as is usually done (Peacock et al. 2001, Hamilton 1998). We illustrate this case in Figure 2.2. More realistically however the effect of the curl term might be determined from simultaneously determining the contributions from both the μ^2 and μ^4 terms. It has not so far been possible from observations which have determined only the μ^2 part (Peacock et al. 2001). On-going survey SDSS galaxy survey has the potential to test this hypothesis. These redshift space effect are nearly independent of the power spectrum of the tangled magnetic field. We discuss below whether it is possible to construct viable models of density power spectrum from tangled magnetic field.

For our calculations we take the magnetic field power spectrum to be power law:

$$B^2(k) = Ak^n \tag{2.33}$$

We consider the range of k between $k_{\rm min}$, which is taken to be zero unless specified otherwise, and the approximate scale at which the alfv́en waves damp in the pre-recombination era (Jedamzik, Katalinic, Olinto 1998, Subramanian & Barrow 1998). Following Jedamzik et al. (1998), $k_{\rm max} \simeq 60\,{\rm Mpc}^{-1}(B_0/(3\times10^{-9}\,{\rm G})$. B_0, the RMS of magnetic field fluctuations at the present epoch, is defined as:

$$B_0^2 \equiv \langle B_i(\mathbf{x},t_0)B_i(\mathbf{x},t_0)\rangle = \frac{1}{\pi^2}\int_0^{k_c} dk k^2 B^2(k) \tag{2.34}$$

Here $k_c = 1\,h\,{\rm Mpc}^{-1}$ (Subramanian & Barrow 2002). This gives:

$$A = \frac{\pi^2(3+n)}{k_c^{(3+n)}}B_0^2 \tag{2.35}$$

2.4 Power Spectrum in Real Space

In the previous subsection, we discussed the redshift space effects in the observed power spectrum. Such effects are nearly independent of the power spectrum of the tangled magnetic

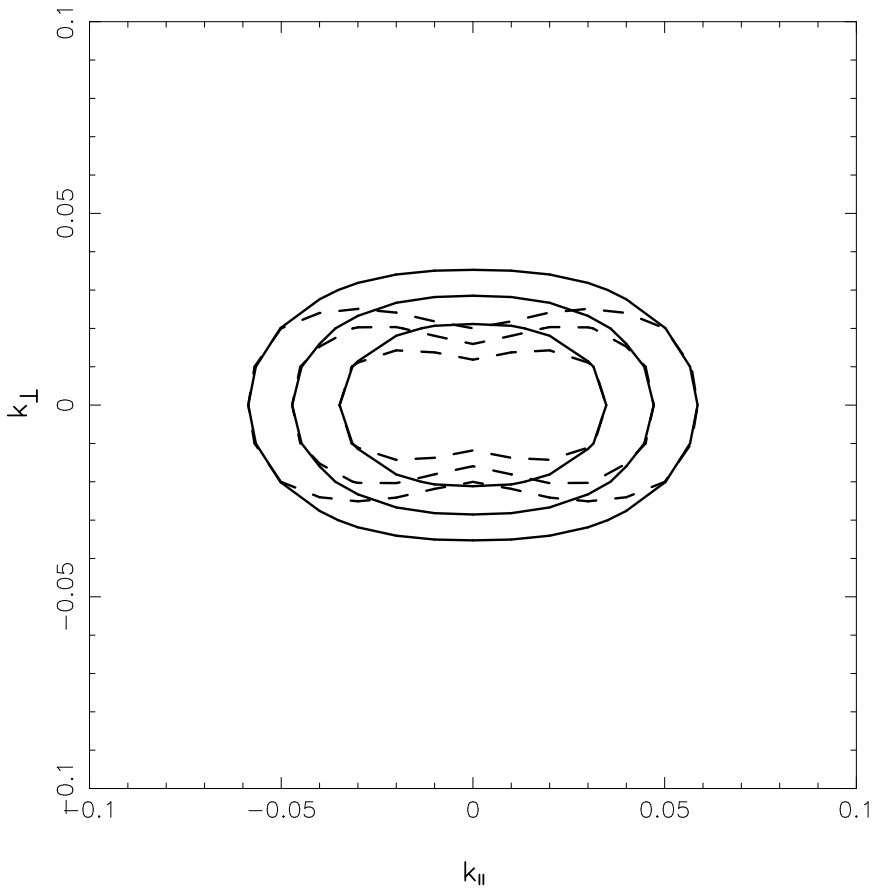

Figure 2.2: Equal redshift space power spectrum contours are shown. The x- and y-axis correspond to the component of k vector parallel and perpendicular to the line of sight. The solid contours show the contours for $\beta = 0.4$, to match with observations (Peacock *et al.* 2001), with zero curl contribution. The dashed curves corresponds to $\beta = 0$ with curl component normalized to give the same quadrupole as in the previous case. Note strong distortions of the curves from the dominant hexadecapole in this case. The contour levels and overall normalization is arbitrary.

field. In this section we study the possibility of constructing viable models of density power spectrum from tangled magnetic fields.

It is conceivable that tangled magnetic fields originated in the very early universe during inflationary epoch (Turner & Widrow 1988, Ratra 1992). In this case tangled magnetic fields can have large coherence lengths, or $k_{\rm min} \simeq 0$ in Eq. (2.33). On the other hand magnetic fields could be of more recent origin ($z \lesssim 10$). However, recent astrophysical processes do not generate large scale magnetic fields. Quasar outflows (see e.g. Furlanetto & Loeb 2001) might pollute the the intergalactic medium sufficiently for it to have magnetic fields with maximum coherence scales $\simeq 2\,$Mpc with magnitudes $\simeq 10^{-9}\,$G. In both cases magnetic fields can have appreciable effect on the large scale structure in the universe at linear scales. We discuss both these possibilities below.

2.4.1 Primordial Magnetic Fields

In this section we discuss the behaviour of the induced matter power spectrum for the scenario in which the magnetic fields might have been generated prior to recombination. Kim, Olinto, and Rosner (1996) calculated the density power spectrum in the presence of tangled magnetic fields. They concluded that for magnetic field power spectrum index $4 < n < -1$, the density power spectrum scales as k^4. We confirm their result but also consider smaller values of n. The observed power spectrum (Spergel *et al.* 2003) is consistent with $P(k) \propto k$ at large scales ($k \lesssim 0.002$); at smaller scales $P(k)$ turns around and scales as k^p with p changing from 0 to -3 as the scales become smaller (see e.g. Efstathiou 1996, Percival *et al.* 2001; Figure 2.3). This clearly means that none of the magnetic field power spectrum index n studied by Kim et al. (1996) can explain the data, which they also pointed out. To make atleast the slope of $P(k)$ agree with the large scale structure data, one needs to consider smaller value of n. For $n = -2$, $P(k) \propto k^3$, for $n \lesssim -2.5$, the power spectrum turns even shallower and we asymptotically approach a scale-invariant spectrum $P(k) \propto k^1$, for $n \sim 3$. An analytical understanding of this behaviour is given in Appendix A (Eq. (2.43)). We consider $n = -2.9$, also studied by Subramanian & Barrow (2002); for this value $P(k)$ scales approximately as k. This suggests that the parameter range of interest lies around this value.

As we discussed above, redshift space effects do not change this conclusion. Subramanian & Barrow (2002) showed that the nearly scale invariant model can lead to CMBR anisotropies $\simeq 10\,\mu$k for angular scales $1000 < \ell < 2000$ for $B_0 = 3 \times 10^{-9}\,$,G. This is comparable to the observed anisotropies at these scales (Mason *et al.* 2002). We check if this model, with this normalization, can give reasonable effect on the large scale structure at the present epoch. We plot in Figure 2.3 the density power spectra for several values of n. The power spectrum for this model is nearly two orders of magnitude below the observed power spectrum at linear scales. Therefore, even though this model leads to the correct

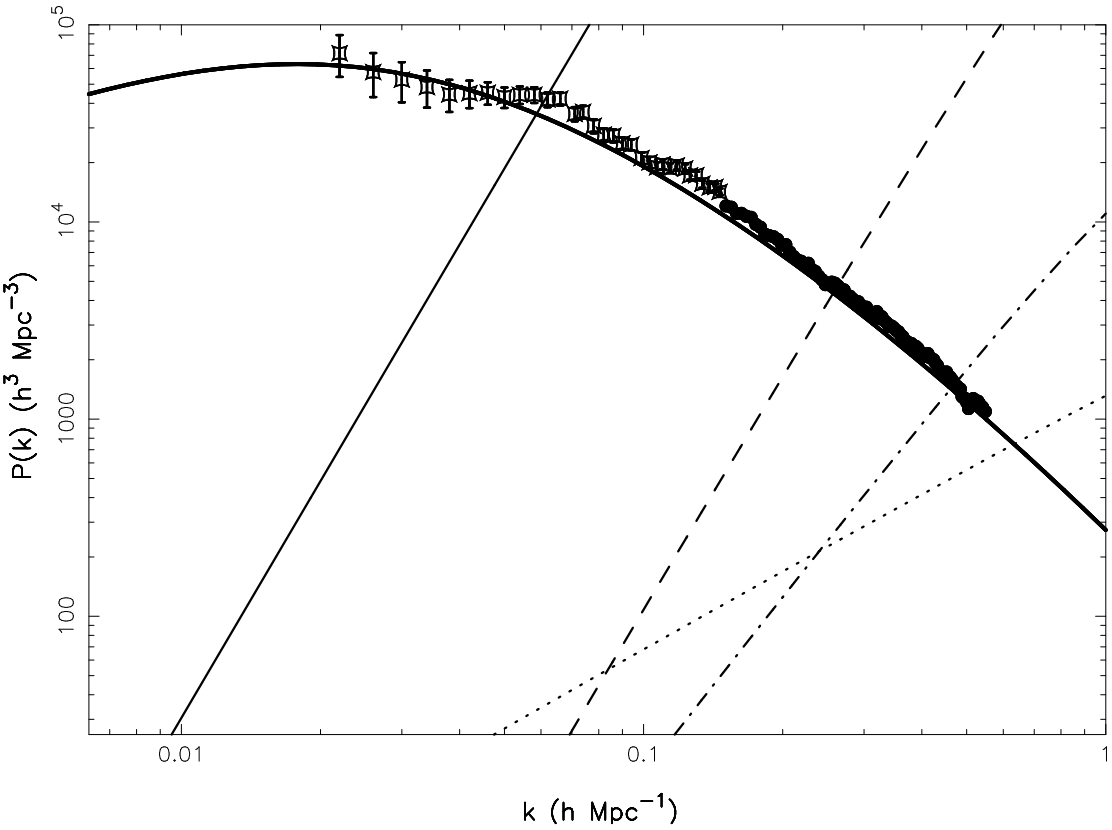

Figure 2.3: The density power spectrum from tangled magnetic fields is shown along with recent observation of the power spectrum from 2dF galaxy survey (Percival *et al.* 2001) and a variant of CDM model. For all the curves $B_0 = 3 \times 10^{-9}$ G. The curves correspond to different values of n: $n = 0$ (Solid line), $n = -1$ (dashed line), $n = -2$ (dot-dashed line), and $n = -2.9$ (dotted line). The thick solid line corresponds to CDM model for a spatially flat universe: $\Omega_m = 0.3$, $\Omega_\Lambda = 0.7$, $\Omega_b = 0.04$.

shape of power spectrum at large scales, the normalization needed to give the correct CMBR anisotropy level is too low. This result is nearly independent of the upper cut-off $k_{\rm max}$ of the magnetic field power spectrum. Figure 2.3 also shows that spectral indices $n \gtrsim -1$ are ruled out by the present data for $B_0 = 3 \times 10^{-9}$ G. However the results for models with $n \gtrsim -1.5$ are strongly dependent on $k_{\rm max}$ and therefore less reliable and they are also likely to give unacceptably large CMBR anisotropies. Therefore we are led to conclude that if tangled magnetic fields existed at the last scattering surface, they are unlikely to have much impact on the large scale structure in the universe at present at linear scales. It should however be noted from Figure 2.3 that magnetic fields can have significant effect on the non-linear scales; which in particular will lead to early collapse of structures. This may have important implications for the re-ionization of the universe (Sethi & Subramanian, 2005).

2.4.2 Low Redshift Magnetic Fields

Another possible scenario is that large-scale magnetic fields could have originated through astrophysical processes at low redhsifts. In this section we evaluate the induced density power spectrum for such a scenario. We consider a simple model to assess the effect of such low redshift magnetic fields on the large scale structure. We assume these fields were created in the post-reionization epoch $z \lesssim 15$ (Spergel *et al.* 2003) and $k_{\rm min} = 6{\rm h\,Mpc}^{-1}$ and $k_{\rm max} = 30{\rm h\,Mpc}^{-1}$, which corresponds roughly to scales between $1\,{\rm h}^{-1}$Mpc and $200\,{\rm h}^{-1}$kpc. The slope of the magnetic field power spectrum and its strength is to be determined by observations. While our choice of $k_{\rm min}$ is motivated by the requirement that astrophysical processes are unlikely to generate larger scale magnetic fields, our choice of $k_{\rm max}$ is largely arbitrary. Our interest is in studying the effect of these fields at scales that are linear at present, i.e. $k \lesssim 0.2\,{\rm Mpc}$. We show in Appendix A (Eq. (2.44) that models in which $k \ll k_{\rm min}$ generically give density power spectrum $\propto k^4$, irrespective of the slope of the tangled magnetic field power spectrum n. For $n \gtrsim -1.5$, the density power spectrum is dominated by the upper cut-off $k_{\rm max}$; in the other limit $k_{\rm min}$ determines the amplitude of the power spectrum. In Figure 2.4, we show the power spectrum for two values of n for $B_0 = 10^{-9}$ G.

For simplicity we take $f(t_0) = 5$. It is seen that if $n \gtrsim 1$ the density power spectrum at linear scales can get appreciable contribution from tangled magnetic fields. However results for these spectral indices depends strongly on the upper cut-off $k_{\rm max}$ and therefore are less reliable. Note that the value of B_0 needed to cause sufficient effect on the large scale structure is quite different from Sethi (2003). This is owing to the fact that $k_{\rm max}$ was taken to be $1\,{\rm hMpc}^{-1}$ in that work and fields were assumed to be locally generated, i.e. $f(t_0) = 1$.

A possible criticism of our analysis is the use of linear theory and neglect of the RHS of Eq. (2.4). Even though we are interested in density perturbations at linear scales at present, presence of the RHS of Eq. (2.4) mixes all modes of tangled magnetic fields and the ve-

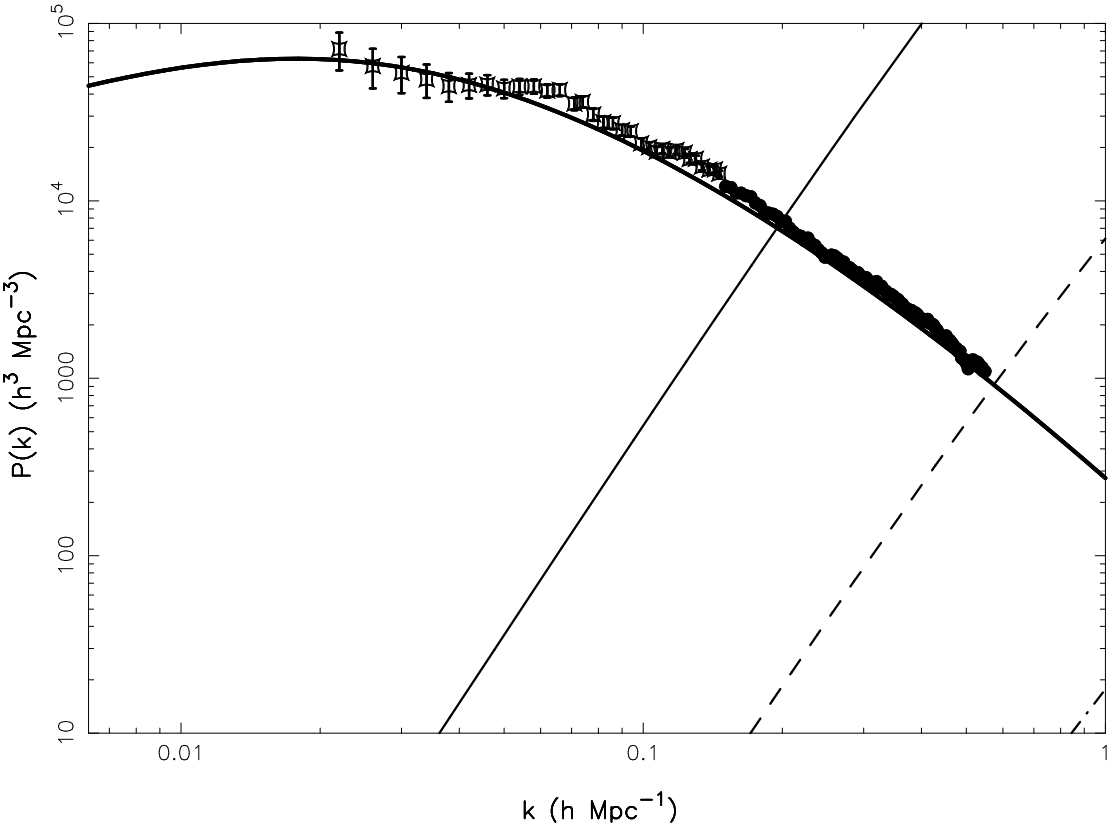

Figure 2.4: Same as Figure 2.3 for the model in which the tangled magnetic fields originate at $z \lesssim 10$ (see text for detail). $B_0 = 10^{-9}$ G and the curves correspond to different spectral index values: $n = 2$ (Solid line), $n = 1$ (dashed line).

locity perturbations and in general cannot be neglected. Our preliminary calculations show that these terms are of order k times the velocity and magnetic field, which means that back reaction of velocity perturbations on the magnetic fields is of higher order than the density power spectrum and could be dropped for studying linear scales. In particular these terms can be neglected if the density perturbation $\delta(\mathbf{k})$ is negligible for all scales in question. The smallest scale at which perturbations can collapse is the magnetic Jeans length $\simeq 100\,\mathrm{kpc}(B_0/(10^{-9}\,\mathrm{G}))$ (Subramanian & Barrow 1998). In practice it is however seen that neglect of non-linear terms to study perturbations at linear scales holds for a wide range of linear scales. For example the use of linear theory in the usual CDM model give reasonable results for studying perturbationsfor $k \lesssim 0.2\,\mathrm{h^{-1}Mpc}$ which are quasi-linear at present, even though smaller structures could have collapsed at much higher redshifts. One case in which we are justified in neglecting the non-linear terms is when the final result can be shown to be nearly independent of the contribution of large k modes of the magnetic field. This as we discussed above is valid for $n \lesssim -1.5$ if the magnetic fields are generated in the early universe. In other cases neglect of this term should depend of both B_0 and n.

2.5 Conclusions

In this chapter we studied the effect of tangled magnetic fields on the large scale structure in the universe. We calculated the power spectrum of the tangled magnetic fields and compared it with the observations at the present epoch. Our results can be summarized as:

1. If the magnetic field originated in the very early universe. It is possible to construct models in which the shape of density power spectrum $\propto k$, i.e. it agrees with the observed power spectrum shape for $k \lesssim 0.02\,\mathrm{h^{-1}\,Mpc^{-1}}$. However compatibility with observed CMBR anisotropies suggests that the density power spectrum from tangled magnetic field is smaller than the observed power spectrum by atleast two orders of magnitudes at linear scales ($k \lesssim 0.2\,\mathrm{h^{-1}\,Mpc^{-1}}$) at present. Therefore very early universe tangled magnetic fields are unlikely to have important impact on the structures in the present universe.

2. We consider a simple model in which the magnetic field were generated with coherence scales $k \gtrsim 2\,\mathrm{h^{-1}\,Mpc^{-1}}$ in the post-reionization epoch $z \lesssim 10$. In all such models the density power spectrum $\propto k^4$, i.e. the shape of the power spectrum is incompatible with the shape of the observed shape. It is possible to construct models in which magnetic field can have important contribution to the density power spectrum for $B_0 \simeq 10^{-9}\,\mathrm{G}$. (It should be noted that the density power spectrum from initial conditions which could have originated during inflation adds to the magnetic field-induced

density power spectrum as the density fields generated by these two processes are uncorrelated; see Eq. (2.11) and the discussion following it.) However these results are quite sensitive to the shape and the upper k cut-off of the tangled magnetic fields power spectrum, which are difficult to fix from either observations or theory.

3. The redshift space effects from tangled magnetic fields have additional features owing to curl component of velocities generated by these fields. The curl component increases both the quadrupole (μ^2 term), hexadecapole (μ^4 term) of the redshift space power spectrum. For very early universe magnetic fields the curl component decays so it cannot have important contribution to the redshift space effects. For magnetic fields generated in the more recent epoch, the curl component of the velocity field can be comparable to the divergence component. In this case both quadrupole and hexadecapole can be dominated by the curl component as opposed to the usual case of divergence collapse. This leads to the interesting possibility that most of the redshift space effects come from the curl component, and the usual way of determining Ω_m from the redshift space distortion is not entirely valid (Peacock *et al.* 2001). As noted above the density power spectrum from tangled magnetic field can dominate the observed power spectrum for $B_0 \simeq 10^{-9}$ G, and hence can be used to probe tangled fields which are too small to be detected by other methods (see e.g. Sethi 2003)

Tangled magnetic fields are unlikely to have provided the initial conditions for the formation of presently-observed structure in the universe. In this chapter we showed that this conclusion seems inevitable for magnetic fields generated in the very early universe.

Appendix A

In this Appendix, we derive expressions for $P(k), \langle\delta(\mathbf{k})v_z(\mathbf{k})\rangle, \langle(v_z(\mathbf{k}))^2\rangle$ and also make an approximate analytical estimate of the small k-dependance of P(k). The real space spatial density contrast and peculiar velocity component along the line of sight are given as:

$$\begin{aligned} \delta(\mathbf{x}) &= \nabla\cdot[\mathbf{B}\times(\nabla\times\mathbf{B})] \\ \mathbf{v}(\mathbf{x})\cdot\hat{\mathbf{z}} &= [\mathbf{B}\times(\nabla\times\mathbf{B})]\cdot\hat{\mathbf{z}} \end{aligned} \tag{2.36}$$

Here $B \equiv B(\mathbf{x}, t_0)$, i.e. the value of magnetic field at the present epoch. The Fourier space expressions for the above fields are:

$$\delta(\mathbf{k}) = \int d^3k_1[(\mathbf{k_1}\cdot\mathbf{B}(\mathbf{k}-\mathbf{k_1}))\,(\mathbf{k}\cdot\mathbf{B}(\mathbf{k_1})) - (\mathbf{k_1}\cdot\mathbf{k})\,(\mathbf{B}(\mathbf{k_1})\cdot\mathbf{B}(\mathbf{k}-\mathbf{k_1}))] \tag{2.37}$$

$$\mathbf{v}(\mathbf{k}) = -i\int d^3k_1[(\mathbf{B}(\mathbf{k_1})\cdot\mathbf{B}(\mathbf{k}-\mathbf{k_1}))\mathbf{k_1} - (\mathbf{k_1}\cdot\mathbf{B}(\mathbf{k}-\mathbf{k_1}))\mathbf{B}(\mathbf{k_1})] \tag{2.38}$$

The volume element in the integrals can be simplified by choosing **k** to lie along the z-axis and $\hat{n}$ to lie in the x-z plane. We thus have,

$$\int d^3k_1 = \int dk_1 k_1^2 \int d\mu \int d\phi \tag{2.39}$$

Here, $\mu \equiv \cos\ \theta$ (θ is the angle between k_1 and the z-axis) while ϕ is the azimuthal angle. In the integral, k_1 ranges from k_{min} to k_{max}, μ from -1 to +1 and ϕ from 0 to 2π. Care has to be taken while evaluating multiple integrals formed from above (for e.g. $\langle\delta^2\rangle$) since the presence of terms like $\delta(k_2 + k - k_1)$ after integrating over k_2 puts a constraint on the integration range of θ as well. Taking all this into account we can split the integration ranges for the cases of interest in our analysis as follows:

For $k_{min} = 0$ and $0 < k_1 < k_{max}$,

$$\int d^3k_1 = \int_0^k dk_1 \int_{-1}^{+1} d\mu + \int_k^{k_{max}-k} dk_1 \int_{-1}^{+1} d\mu + \int_{k_{max}-k}^{k_{max}} dk_1 \int_{\mu_{max}}^{1} d\mu \tag{2.40}$$

For $k_{min} \neq 0$ and $0 < k_1 < k_{min}$,

$$\int d^3k_1 = \int_{k_{min}}^{k+k_{min}} dk_1 \int_{-1}^{\mu_{min}} d\mu + \int_{k+k_{min}}^{k_{max}-k} dk_1 \int_{-1}^{+1} d\mu + \int_{k_{max}-k}^{k_{max}} dk_1 \int_{\mu_{max}}^{1} d\mu \tag{2.41}$$

where $\mu_{max} = (k^2 + k_1^2 - k_{max}^2)/(2kk_1)$ and $\mu_{min} = (k^2 + k_1^2 - k_{min}^2)/(2kk_1)$

To calculate P(k) we take the ensemble average of $[\delta(\mathbf{k})]^2$. This product contains terms involving four point functions of **B**. By assuming that **B** is Gaussian distributed in the ensembles such terms can be written as sums of products of two-point functions of **B**. Finally using Eq. (2.8) and simplifying, we arrive at the following expression for P(k):

$$P(k) = \int_{k_{min}}^{k_{max}} dk_1 \int_{-1}^{+1} d\mu \frac{B^2(k_1)B^2(|\mathbf{k} - \mathbf{k_1}|)}{|\mathbf{k} - \mathbf{k_1}|^2} [2k^5k_1^3\mu + k^4k_1^4(1 - 5\mu^2) + 2k^3k_1^5\mu^3] \tag{2.42}$$

We evaluate this double integral numerically. However we can analytically see the form for P(k) when $k \ll k_{\rm max}$ both for $k_{\rm min} = 0$ as well as $k_{min} \neq 0$ as follows:

For $k_{\rm min} = 0$ and $k \ll k_{\rm max}$, the relevant case when the magnetic fields originate in the early universe, the only major contribution to the $P(k)$ comes from the second integral in Eq. (2.40). We thus have to lowest order in $k/k_{\rm max}$,

$$P(k) \sim Ak^{2n+7} + Bk_{\rm max}^{2n+3}k^4 + Ck_{\rm max}^{2n+1}k^6 + ...(\text{higher powers of k}) \tag{2.43}$$

where, A,B and C are coefficients depending only on n. We thus see that for $n > -1.5$ the leading order term is proportional to k^4 whereas for $n < -1.5$ it is proportional to k^{2n+7}. In particular for $n = -2$, the dependance goes as k^3. Also, $P(k) \to k^1$ as $n \to -3$.

For $k_{min} \neq 0$ and $k \ll k_{min}$, the case if the magnetic fields are of more recent origin, the leading contribution to $P(k)$ comes from the third integral in Eq. (2.41). Thus, to lowest order in k we get,

$$P(k) \sim Ak^4(k_{\rm max}^{2n+3} - k_{\rm min}^{2n+3}) + ...(\text{higher powers of k}) \tag{2.44}$$

Thus, we see that with an infrared cutoff which is much larger than the wavenumber of interest, the dependance of $P(k)$ is generically k^4. The dependance on $k_{\rm max}$ and $k_{\rm min}$ is such that for $n > -1.5$, the value of $P(k)$ is determined by and increases with $k_{\rm max}$. In the otherlimit $P(k)$ is determined by $k_{\rm min}$. We now evaluate the correlation $\langle \delta(k)\, \mathbf{v} \cdot \hat{\mathbf{z}} \rangle$ We can show that it is simply proportional to P(k) in the following way: From the assumptions of homogeneity and isotropy, we can write

$$\langle v_i(\mathbf{k}) v_j(\mathbf{q}) \rangle = \left(A(k^2)\, \delta_{ij} + B(k^2)\, k_i k_j \right)\, \delta^3(\mathbf{q} - \mathbf{k}) \tag{2.45}$$

where $A(k^2)$ and $B(k^2)$ are some as yet undetermined coefficients. Thus, using the continuity equation, Eq. (2.2):

$$\langle \delta(\mathbf{k})\, \mathbf{v}(\mathbf{k}) \cdot \hat{\mathbf{n}} \rangle = -i \langle k_i v_i v_j n_j \rangle = -i \mathbf{k} \cdot \hat{\mathbf{n}} [A(k^2) + k^2 B(k^2)] \tag{2.46}$$

Similarly we get,

$$P(k) \equiv -\langle k_i v_i k_j v_j \rangle = -k^2 [A(k^2) + k^2 B(k^2)] \tag{2.47}$$

Thus from these equations we get the following relation:

$$\langle \delta(\mathbf{k})\, \mathbf{v}(\mathbf{k}) \cdot \hat{\mathbf{n}} \rangle = i \frac{\mathbf{k} \cdot \hat{\mathbf{n}}}{k^2}\, P(k) \tag{2.48}$$

From this derivation Eq. (2.30) follows. Finally, this allows us to write $\langle (\mathbf{v}(\mathbf{k}) \cdot \hat{\mathbf{n}})^2 \rangle$ correlation:

$$\begin{aligned} \langle (\mathbf{v}(\mathbf{k}) \cdot \hat{\mathbf{n}})^2 \rangle &= \int_{k_{min}}^{k_{max}} dq \int_{-1}^{+1} d\mu \frac{B^2(q) B^2(|\mathbf{k} - \mathbf{q}|)}{|\mathbf{k} - \mathbf{q}|^2} \left[\cos^2\alpha \left(2k^3 q^3 \mu - 5k^2 q^4 \mu^2 \right.\right. \\ &+ \left.\left. k^2 q^4 - q^5 k(\mu - 3\mu^3) \right) + q^5 k(\mu - \mu^3) \right] \end{aligned} \tag{2.49}$$

Here, α is the angle between $\mathbf{k}$ and $\hat{n}$.

Bibliography

Barrow J.D., Ferreira P.G., & Silk J., 1997, Phys. Rev. Lett., 78, 3610

Blasi P., Burles S., Olinto A.v., 1999, ApJ, 514, 79L

Colless M. et al. , 2001, MNRAS, 328, 1039

Efstathiou G., in Schaeffer R., Silk J., Spiro M., & Zinn-Justin J., 1996, ASP Conf. Ser. 24: Cosmology and Large-scale Structure in the Universe

Furlanetto S.R. & Loeb A., 2001, ApJ, 556, 619

Hamilton A.J.S., 1998, ASSL Vol. 231: The Evolving Universe, 185

Hawkins E. et al. , 2002, MNRAS, 346, 78

Hatton S. & Cole S., 1998, MNRAS, 296, 10

Jedamzik K., Katalinić V., & Olinto A.V., 2000, Phys. Rev. Lett., 85, 700

Jedamzik K., Katalinić V., & Olinto A. V., 1998, Phys. Rev. D., 57, 3264

Kaiser N., 1987, MNRAS, 227, 1

Kim E., Olinto A.V., & Rosner R., 1996, ApJ, 468, 28

Kim K.-T., Kronberg P. P., Giovannini G., & Venturi T., 1989, Nature, 341, 720

Kosowsky A. & Loeb A., 1996, ApJ, 469, 1

Kronberg P. P., 1994, Reports on Progress in Physics, 57, 325

Kronberg P. P. & Simard-Normandin M., 1976, Nature, 263, 653

Lahav O. et al. , 2002, MNRAS, 333, 961

Lahav O., Rees M. J., Lilje P. B., & Primack J. R. 1991, MNRAS, 251, 128

Landau L. D. & Lifshitz E. M. 1987, Fluid Mechanics, Pergamon Press

Mason B. S. et al. , 2002, ApJ, 591, 540

Parker E.N., 1979, Oxford, Clarendon Press; New York, Oxford University Press, 1979, 858

Peebles P. J. E., 1980, Large Scale Structure of the Universe, Princeton University Press, 435

Peacock J. A. et al. , 2001, Nature, 410, 169

Perlmutter S. et al. , 1999, ApJ, 517, 565

Percival W. J. et al. , 2001, MNRAS, 327, 1297

Ratra B., 1992, ApJ Lett., 391, L1

Rees M. J. & Reinhardt M., 1972, A & A, 19, 189

Riess A. G. et al. , 1998, Astron. Journal , 116, 1009

Ruzmaikin A.A., Shukurov A.M., Sokoloff D.D., *Magnetic Fields of Galaxies*, Kluwer, Dordrecht (1988)

Sethi S. K., 2003, MNRAS, 342, 962

Spergel D. N. et al. , 2003, ApJS, 148, 175

Subramanian, K. & Barrow, J. D. 2002, MNRAS, 335, L57

Sethi & Subramanian, 2005, MNRAS, 356, 778

Subramanian K. & Barrow J. D., 1998, Phys. Rev. Lett., 81, 3575

Subramanian K. & Barrow J. D., 1998, Phys. Rev. D., 58, 83502

Tegmark et al. ., 2004, ApJ, 606, 702

Turner M.S. & Widrow L.M., 1988, Phys. Rev. D., 37, 2743

Tytler, D., O'Meara, J. M., Suzuki N., & Lubin D., 2000, Physics Reports, 333, 409

Vallée J. P., 1990, ApJ, 360, 1

Wasserman I., 1978, ApJ, 224, 337

Widrow L. M., 2002, Reviews of Modern Physics, 74, 775

York D. G. et al. , 2000, Astron. Journal , 120, 1579

I. B. Zeldovich, A. A. Ruzmaikin, and D. D. Sokolov, New York, Gordon and Breach Science Publishers (The Fluid Mechanics of Astrophysics and Geophysics. Volume 3), 1983, 381 p.